ChemComm

COMMUNICATION

View Article Online
View Journal | View Issue

Cite this: *Chem. Commun.*, 2025, **61**, 7490

Received 26th June 2024,
Accepted 8th April 2025

DOI: 10.1039/d4cc03125c

rsc.li/chemcomm

Particle size effects on vapour uptake and release dynamics in metal–organic frameworks†

Joshua Nicks, *[a] Cosmin Mudure, [b] Jordan James,[a] Alexander McDougall,[a] William O. H. Hughes, [c] John Spencer, [d] Tina Düren[b] and Andrew D. Burrows *[a]

Reducing the particle size of the metal–organic frameworks (MOFs) MIL-68(In) and ZIF-8 leads to increased adsorption of volatile semiochemical guests. Opposing trends were observed in release dynamics, with the release rate of isobutyl acetate increasing with particle size for MIL-68(In) and decreasing for ZIF-8, which can be attributed to the lower diffusion barriers through channels in comparison to moving between discrete pores.

Metal–organic frameworks (MOFs) are porous materials composed of metal nodes that are interconnected by bridging organic linkers.[1] The exceptional porosities and structural tunability of MOFs have led to their implementation in a range of gas capture,[2,3] separation,[4] and catalytic conversion applications.[5] As such, further understanding of the loading and release dynamics of volatile molecules in MOFs is vital to realising their potential. Previous studies have identified that modifying the structure of a MOF through ligand expansion or functionalisation can tune the diffusion dynamics of guests.[6–8] However, the effect of the particle size on diffusive gas uptake, release, and related applications in MOFs has attracted less attention.

In this study we explore the effects of systematic reduction of the mean particle size of the channel-type MIL-68(In) and the cage-type ZIF-8 MOFs on the uptake and release rates of volatile biological messenger molecules, known generally as semiochemicals. These chemicals can be used to manipulate insect behaviour for sustainable pest management strategies, but their volatility limits their practical utility.[9] Inclusion of these molecules within porous materials is a potential solution to this issue, making them ideal model guests for this study.[10,11]

MIL-68(In) and ZIF-8 were chosen for the ease of control over their particle sizes and for their distinct pore architectures. MIL-68(In) is composed of chains of In(III) octahedra connected by terephthalate linkers to form a kagome lattice (Fig. 1a).[12] The fused nature of these indium octahedra results in one-dimensional trigonal (~6.2 Å, atom-to-atom based on ionic radii) and hexagonal (~16.5 Å) channels separated by terephthalate walls.[12] In contrast, ZIF-8 is composed of Zn(II) tetrahedra interconnected by 2-methylimidazolate linkers to form a sodalite topology, in which large tetrahedral cages (~11.7 Å) are connected to four neighbouring cages *via* shared corners, forming windows of ~3.4 Å, and six small cubic cages *via* shared faces with windows of ~0.8 Å (Fig. 1b).[13,14] The use of both channel- and cage-type MOFs allows us to examine the implications of fundamentally different pore architectures on the loading and release dynamics of guests.

The particle sizes of the as-synthesised frameworks were controlled through two different methods, based on the different donor atoms of each linker. In the case of MIL-68(In), we utilised the standard approach of employing a monotopic modulator, sodium acetate, which acts as a capping agent to restrict the growth of the crystallites.[15,16] Four samples of MIL-68(In) were obtained with distinct particle size ranges by

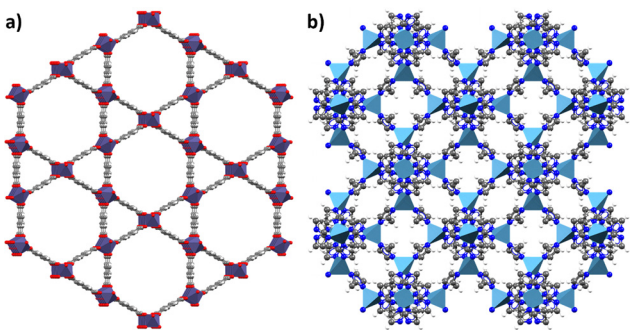

Fig. 1 Crystal structures of (a) MIL-68(In) and (b) ZIF-8. Indium octahedra are shown in purple, zinc tetrahedra in light blue, carbons in grey, nitrogens in dark blue, oxygens in red and hydrogens in white.

[a] *Department of Chemistry, University of Bath, Claverton Down, Bath, BA2 7AY, UK. E-mail: jn694@bath.ac.uk, a.d.burrows@bath.ac.uk*
[b] *Centre for Integrated Materials, Processes and Structures & Department of Chemical Engineering, University of Bath, Claverton Down, BA2 7AY, UK*
[c] *School of Life Sciences, University of Sussex, Falmer, Brighton, BN1 9QJ, UK*
[d] *Chemistry Department, School of Life Sciences, University of Sussex, Falmer, Brighton, BN1 9QJ, UK*

† Electronic supplementary information (ESI) available. See DOI: https://doi.org/10.1039/d4cc03125c

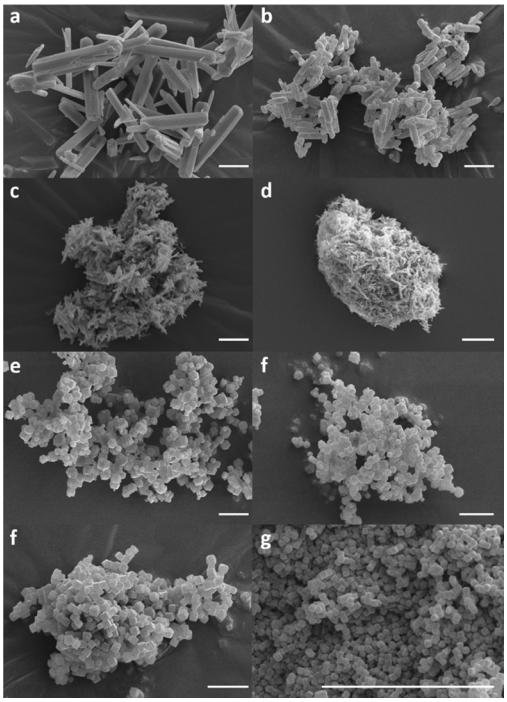

Fig. 2 Scanning electron microscopy images of MIL-68(In) **A–D** and ZIF-8 **E–H** with increasing degrees of modulation down the figure. All scale bars represent 5 μm.

systematically increasing the concentration of modulator, and these are referred to herein as **A**, **B**, **C**, and **D** respectively. All experimental details are provided in the ESI.†

Scanning electron microscopy (SEM) imaging of the activated frameworks shows that increasing the concentration of the modulator decreased both the lengths and widths of the MIL-68(In) rods formed (Fig. 2A–D and Fig. S1–S4, ESI†), whilst powder X-ray diffraction (PXRD) demonstrates that the crystal structure was maintained in each sample (Fig. S5, ESI†). With increasing modulation, there is a preference for the 'through-pore' reflection [2,2,0], over the 'through-wall' [1,1,0] reflection, as the monotopic acetate modulator disproportionately decreases crystallisation in the direction of linker extension. Particle size distributions shown in Fig. S6 and Table S2 (ESI†) demonstrate the significant difference in the particle sizes obtained for each set **A–D**. The unmodulated system, **A**, presents as rods (11.45 ± 3.43 μm) with well-defined edges, but upon introduction of modulator, the particles of **B** are significantly smaller with less clearly defined edges but more consistent particle sizes (3.30 ± 0.90 μm). Further modulation continues to reduce the overall particle sizes for **C** (1.45 ± 0.39 μm) and **D** (1.01 ± 0.27 μm) as well as leading to significant aggregation of the microrods.

The particle sizes of the ZIF-8 system were controlled through a surfactant-mediated synthesis, in which surfactant molecules adsorb onto the surfaces of growing MOF crystallites without bonding, arresting their crystallisation.[17] As such, the surfactant concentration is critical in controlling the end particle size. SEM imaging of the activated frameworks shows that with increasing surfactant concentration the resultant particle size decreases (Fig. 2E–H and Fig. S7–S10, ESI†), evidenced by the particle size distributions shown in Fig. S12 (ESI†). PXRD patterns of each ZIF-8 set also demonstrate that the crystal structure is maintained throughout, with an increased representation of the [2,1,1] reflection over the [1,1,0] as the dimensions decrease, a result of the change in morphology from the larger rhombohedral dodecahedral particles of **E** (1.01 ± 0.69 μm) and **F** (0.92 ± 0.19 μm) to the cubic crystallites observed for samples **G** (0.67 ± 0.13 μm) and **H** (0.18 ± 0.02 μm).

Thermogravimetric analyses (TGA) of the as-prepared and activated samples, and ^{1}H NMR spectra of digested activated samples indicate that activation in a ventilated oven at 120 °C for 72 hours removed all solvent molecules present in the pores post-synthesis (Fig. S13–S18, ESI†), with the crystallinities of the samples maintained (Fig. S19 and S20, ESI†). These analyses also demonstrate that neither modulator remains post-synthesis.

N_2 sorption isotherms were obtained at 77 K for all activated systems (Fig. S21 and S22, ESI†) and used to calculate their BET areas (Table S2, ESI†). The MIL-68(In) samples have proportional levels of defectivity and porosity, a result of the short synthesis times required to produce controlled particle sizes which has been observed in previous reports.[18,19] The ZIF-8 samples show negligible differences in sorption behaviour and surface area, with lower defectivity percentages attributed to the extended synthesis duration. Pore size distributions calculated for both systems from isotherm data demonstrate narrow distributions within each MOF system and similar overall distributions between the two MOFs (Fig. S23 and S24, ESI†), suggesting that only the particle sizes and not the overall porosity of each system should have an effect on uptake and release dynamics.

The systematically decreasing particle size ranges alongside the two distinct pore architectures of both MOF systems present an ideal sample set for studying how particle size affects volatile guest uptake and release. In line with our previous work,[10,11] the volatile guests chosen for loading were the semiochemicals isobutyl acetate and 3-octanone, which have vapour pressures at 20 °C of 13 and 2 mmHg, respectively.

Loading was performed according to our vapour diffusion method, in which activated MOFs are placed in a sealed dry environment with multiple semiochemical wells providing a saturated atmosphere.[11] Semiochemical uptakes for each MOF system are shown in Fig. 3.

The uptakes of both semiochemicals are greater in the MIL-68(In) systems than the ZIF-8 systems, despite the larger pore volumes of the ZIF samples (Fig. S25, S26 and Table S2, ESI†). We attribute this to the difference in diffusion barriers between the two systems, as the open-ended channel pores of MIL-68(In) have a much lower barrier to diffusion than the fused cages and narrow apertures of ZIF-8. The generally lower uptakes of isobutyl acetate compared to 3-octanone in the ZIF system is ascribed to the reduced ability of the former to diffuse through the cage windows, a result of the increased sterics of the

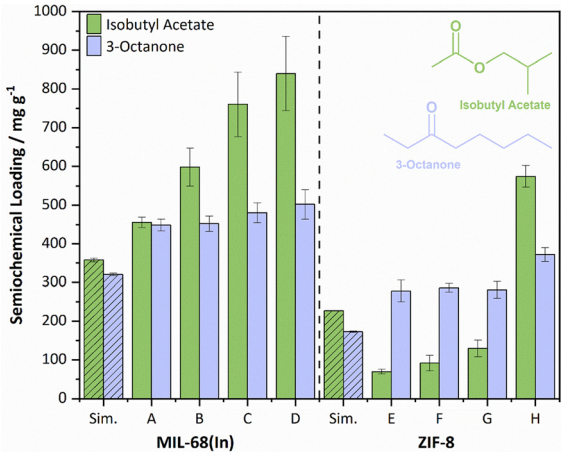

Fig. 3 Isobutyl acetate and 3-octanone semiochemical uptakes for MIL-68(In) **A–D** and ZIF-8 **E–H**, shown alongside simulated uptakes obtained from single point isotherms (hashed bars).

isobutyl group. Similar cases in which slight changes in molecular structure elicit significantly different rates of diffusion through ZIF-8 have previously been demonstrated for xylene isomers,[20] ethane/ethylene,[21] and propane/propylene mixtures,[22] and similar pore aperture effects have been reported for other MOF architectures.[23,24] A report by Ueda and co-workers highlighted that it is the cylindrical cross-sectional diameter of a molecule that is the limiting factor to diffusion through ZIF-8 windows, suggesting that the larger cylindrical diameter of isobutyl acetate restricts the adsorptive uptake.[25] This is further supported by the reduced experimental uptake of isobutyl acetate in ZIF-8 when compared to the simulated uptakes obtained through Grand-Canonical Monte Carlo methods (see Section S1.4 for details, ESI†).

Reducing the particle size in both systems resulted in an increase of the uptake of both semiochemicals, though the effect is larger for isobutyl acetate. This is attributed to the increased surface adsorption associated with the increasing surface area to volume ratios of the smaller particles. This is further evidenced by the generally larger experimental uptakes for all systems compared to the uptakes obtained from simulated single-point isotherms, which cannot account for surface loading. We have observed the enhanced affinity of isobutyl acetate for surface adsorption compared to other semiochemicals previously and ascribe this to its higher volatility and polarity.[11]

To observe differences in the release rates of these semiochemical guests with particle size, we conducted time-resolved release studies. The loaded MOFs were kept in an open vial at a constant temperature of 40 °C and ^{1}H NMR spectra of digested samples were obtained at set time intervals to determine the release profile from each framework over 50 days (Fig. 4). It is clear from Fig. 4a and b that changes in the particle size of both MIL-68(In) and ZIF-8 MOFs have significant effects on the rate of loss of isobutyl acetate from the pores. In MIL-68(In), samples **A–D** have the same loading after 1 day despite different initial loadings, which we ascribe to the loss of surface loaded isobutyl acetate. However, from this point, the release rate increases with particle size, resulting in a loading difference of >100 mg g^{-1} between **A** and **D** after 50 days.

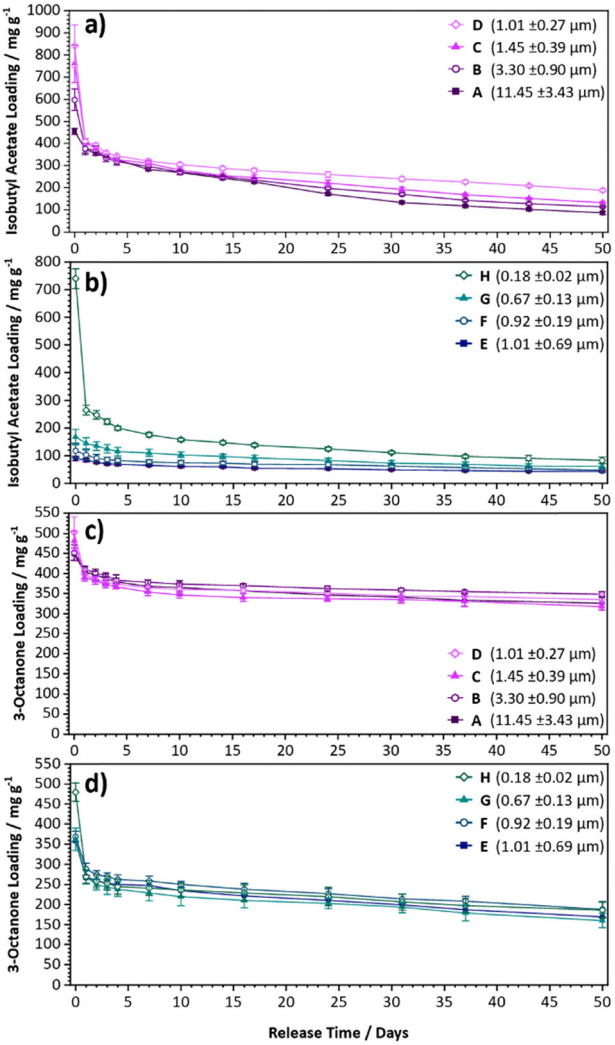

Fig. 4 Semiochemical release profiles for isobutyl acetate from (a) MIL-68(In) and (b) ZIF-8, and 3-octanone from (c) MIL-68(In) and (d) ZIF-8 samples.

ZIF-8 does not follow the same trend as MIL-68(In). A large initial loss of semiochemical at day 1 is observed for the smallest particles of sample **H**, consistent with the loss of surface loaded isobutyl acetate. However, after this point, the rate of release increases with decreasing ZIF-8 particle size. Sample **H** releases over half of its day 1 loading over the duration of the release, whereas sample **E**, with particle sizes an order of magnitude larger, shows negligible release over 50 days.

We attribute this difference in the release dynamics of isobutyl acetate between the two MOFs to the nature of their pores. The channel pores of MIL-68(In) allow for more facile diffusion into and out of the pores through their open-ended nature. Thus, the larger and therefore more ordered particles release isobutyl acetate faster than the smaller aggregated particles which essentially block the pores of adjacent particles. In the case of ZIF-8, there is a more significant energy barrier to diffusion through the cage windows.[20,21] As such, the larger particles load and release much slower than the smaller particles, as the smaller particles contain an increased proportion of

"surface" cages. A number of previous reports have demonstrated that even a small increase in molecular size leads to significant effects on the diffusion rates of guests through ZIF-8 windows.[25,26] In particular, Hupp *et al.* demonstrated that the diffusivities of linear alkanes from C_5 to C_{16} vary from 10^{-14} to 10^{-18} m^2 s^{-1}, with shorter alkanes generally displaying higher diffusivities.[27] As such, the large molecular weight and more significant steric size of isobutyl acetate would be expected to give a lower diffusivity. This is perhaps best evidenced by comparing samples MIL-68(In) **D** and ZIF-8 **E**, which have similar particle size ranges, and demonstrate a significantly higher rate of release from the channel-pored MIL-68(In) system. Moreover, simulated Henry constants (Fig. S41, ESI†) demonstrate that there is a stronger interaction for both semiochemicals with MIL-68(In) than ZIF-8, demonstrating that the strength of adsorption is not a reason for the rates of release within ZIF-8 to be slower.

These differences in release dynamics are not observed for 3-octanone-loaded samples (Fig. 4c and d). Though a similar initial loss of surface-loaded semiochemical after 1 day is observed in both systems, there is no statistically significant difference between the releases after this point. This is a consequence of the much lower volatility of 3-octanone which diminishes the effect of particle size. PXRD measurements of the loaded, post-release and humidity-treated samples demonstrated that the structures of **A–H** were maintained throughout (Fig. S31–S40, ESI†), indicating that any losses of crystallinity were not affecting diffusion dynamics.

To conclude, we conducted semiochemical uptake and release studies to understand how particle size impacts volatile guest behaviour in channel- and cage-type MOFs. Decreasing particle size leads to an increased uptake due to adsorption on the external crystal surfaces, and this effect is more prevalent when the guest is the more volatile isobutyl acetate. Furthermore, the substantial difference in the barrier to diffusion through open channels and cages with small window apertures results in opposing effects of particle size on semiochemical release. For open channel MOFs, reduction of the particle size leads to aggregation and blocking of the release pathways hence slower release, whereas in cage MOFs the window size can inhibit loading into the inner cages of larger crystallites, significantly reducing the rate of guest release.

These results are pertinent in the context of using MOFs for any guest uptake/release application. The inflated uptake values that arise from surface adsorption in cases of smaller particles can lead to misunderstanding when using larger guests, such as the semiochemicals explored in this study. Moreover, the observed differences in the effects of particle size on release from both the channel and cage systems has significant implications for the selections of MOF architectures for applications such as purification, molecular separations, and guest delivery.

The authors thank the Leverhulme Trust (RPG-2019-009), the EPSRC Centre for Doctoral Training in Advanced Automotive Propulsion Systems (EP/S023364/1), and the University of Bath for financial support and acknowledge the MC^2 facility at the University of Bath for technical support.

Data availability

The data supporting this article have been included as part of the ESI.†

Conflicts of interest

There are no conflicts to declare.

References

1 H. Furukawa, K. E. Cordova, M. O'Keeffe and O. M. Yaghi, *Science*, 2013, **341**, 1230444.
2 K. Sumida, D. L. Rogow, J. A. Mason, T. M. McDonald, E. D. Bloch, Z. R. Herm, T.-H. Bae and J. R. Long, *Chem. Rev.*, 2012, **112**, 724–781.
3 E. Martínez-Ahumada, M. L. Díaz-Ramírez, M. de J. Velásquez-Hernández, V. Jancik and I. A. Ibarra, *Chem. Sci.*, 2021, **12**, 6772–6799.
4 Q. Qian, P. A. Asinger, M. J. Lee, G. Han, K. Mizrahi Rodriguez, S. Lin, F. M. Benedetti, A. X. Wu, W. S. Chi and Z. P. Smith, *Chem. Rev.*, 2020, **120**, 8161–8266.
5 M. Ding, R. W. Flaig, H.-L. Jiang and O. M. Yaghi, *Chem. Soc. Rev.*, 2019, **48**, 2783–2828.
6 T. M. Osborn Popp, A. Z. Plantz, O. M. Yaghi and J. A. Reimer, *ChemPhysChem*, 2020, **21**, 32–35.
7 A. C. Forse, K. A. Colwell, M. I. Gonzalez, S. Benders, R. M. Torres-Gavosto, B. Blümich, J. A. Reimer and J. R. Long, *Chem. Mater.*, 2020, **32**, 3570–3576.
8 T. Maity, P. Malik, S. Bawari, S. Ghosh, J. Mondal and R. Haldar, *Nat. Commun.*, 2023, **14**, 2212.
9 J. G. Logan and M. A. Birkett, *Pest Manage. Sci.*, 2007, **63**, 647–657.
10 H. Amer Hamzah, D. Rixson, J. Paul-Taylor, H. V. Doan, C. Dadswell, G. W. Roffe, A. Sridhar, C. L. Hobday, C. Wedd, T. Düren, W. O. H. Hughes, J. Spencer and A. D. Burrows, *Dalt. Trans.*, 2020, **49**, 10334–10338.
11 J. Nicks, G. C. Shearer, J. Paul-Taylor, J. Lai-Morrice, C. Dadswell, D. Guest, W. O. H. Hughes, J. Spencer, T. Düren and A. D. Burrows, *Chem. – A Eur. J.*, 2024, e202401407.
12 C. Volkringer, M. Meddouri, T. Loiseau, N. Guillou, J. Marrot, G. Férey, M. Haouas, F. Taulelle, N. Audebrand and M. Latroche, *Inorg. Chem.*, 2008, **47**, 11892–11901.
13 K. S. Park, Z. Ni, A. P. Côté, J. Y. Choi, R. Huang, F. J. Uribe-Romo, H. K. Chae, M. O'Keeffe and O. M. Yaghi, *Proc. Natl. Acad. Sci. U. S. A.*, 2006, **103**, 10186–10191.
14 C. L. Hobday, C. H. Woodall, M. J. Lennox, M. Frost, K. Kamenev, T. Düren, C. A. Morrison and S. A. Moggach, *Nat. Commun.*, 2018, **9**, 1429.
15 R. S. Forgan, *Chem. Sci.*, 2020, **11**, 4546–4562.
16 L.-N. Jin, Q. Liu and W.-Y. Sun, *CrystEngComm*, 2013, **15**, 4779–4784.
17 Y. Pan, D. Heryadi, F. Zhou, L. Zhao, G. Lestari, H. Su and Z. Lai, *CrystEngComm*, 2011, **13**, 6937–6940.
18 C. Duan, F. Li, M. Yang, H. Zhang, Y. Wu and H. Xi, *Ind. Eng. Chem. Res.*, 2018, **57**, 15385–15394.
19 N. Al-Janabi, X. Fan and F. R. Siperstein, *J. Phys. Chem. Lett.*, 2016, **7**, 1490–1494.
20 D. M. Polyukhov, A. S. Poryvaev, A. S. Sukhikh, S. A. Gromilov and M. V. Fedin, *ACS Appl. Mater. Interfaces*, 2021, **13**, 40830–40836.
21 S. Berens, F. Hillman, H.-K. Jeong and S. Vasenkov, *Microporous Mesoporous Mater.*, 2019, **288**, 109603.
22 H. T. Kwon and H.-K. Jeong, *J. Am. Chem. Soc.*, 2013, **135**, 10763–10768.
23 X. Wu, Y. Gao and J. Bi, *Microporous Mesoporous Mater.*, 2024, **363**, 112827.
24 S. Song, C. Liu, R. Ding, X. Gao, M. Wang, Z. Li and X. Zhao, *J. Solid State Chem.*, 2022, **314**, 123376.
25 T. Ueda, T. Yamatani and M. Okumura, *J. Phys. Chem. C*, 2019, **123**, 27542–27553.
26 D. Peralta, G. Chaplais, J.-L. Paillaud, A. Simon-Masseron, K. Barthelet and G. D. Pirngruber, *Microporous Mesoporous Mater.*, 2013, **173**, 1–5.
27 C. O. Audu, D. Chen, C.-W. Kung, R. Q. Snurr, S. T. Nguyen, O. K. Farha and J. T. Hupp, *Langmuir*, 2021, **37**, 9405–9414.